

## Surface segregation of conformationally asymmetric polymer blends

Semjon Stepanow and Andrei A. Fedorenko

*Fachbereich Physik, Martin-Luther-Universität Halle, D-06099 Halle, Germany*

(Received 2 November 2005; published 2 March 2006)

We have generalized the Edwards' method of collective description of dense polymer systems in terms of effective potentials to polymer blends in the presence of a surface. With this method we have studied conformationally asymmetric athermal polymer blends in the presence of a hard wall to the first order in effective potentials. For polymers with the same gyration radius  $R_g$  but different statistical segment lengths  $l_A$  and  $l_B$  the excess concentration of stiffer polymers at the surface is derived as  $\delta\rho_A(z=0) \sim (l_B^2 - l_A^2) \ln(R_g^2/l_c^2)$ , where  $l_c$  is a local length below of which the incompressibility of the polymer blend is violated. For polymer blends differing only in degrees of polymerization the shorter polymer enriches the wall.

DOI: [10.1103/PhysRevE.73.031801](https://doi.org/10.1103/PhysRevE.73.031801)

PACS number(s): 61.25.Hq, 68.47.Pe, 83.80.Tc

### I. INTRODUCTION

The effects of surfaces on the behavior of polymer melts and blends is of basic importance in their numerous applications such as adhesion, lubrication, wetting, catalysis, etc. [1]. The structure and properties of the blends and other polymeric materials within a few nanometers at a surface can differ significantly from corresponding properties in the bulk. For example, in polymer blend a segregation of one of the components to the surface is possible even if the blend is miscible in bulk. Hence the questions how the surface can change the properties of polymeric materials and how it may be controlled are of practical interest. Despite the large theoretical and experimental interest in the behavior of polymer blends in the presence of surfaces and achieved basic understanding there is no satisfactory analytical treatment of segregation of polymers at surfaces. Most studies of polymer blends near surfaces are based on phenomenological expressions for a free energy, which include surface terms that account for adsorption or repulsion of a particular type of monomers [2,3]. Minimization of the free energy gives equilibrium concentration profiles for each component. There exist more rigorous approaches, which allow one to derive the concentration profiles starting from the microscopic polymer statistics in the presence of a surface. One of such microscopic approaches is the integral equations method which can be applied to various site-site or hard-particle models of a dense polymeric system [4]. This method having many advantages such as ability to predict microscopic correlations between different types of monomers and between monomers and surfaces requires a considerable amount of numerical computations. Most of analytically treatable methods, which rely on the continuum Gaussian chain model, take into account the monomer-monomer interactions usually using either the random phase approximation [5], which is most suited to treat systems in the weak segregation limit or self-consistent field theories [6,7], which are most suited to treat systems in the strong segregation limit.

Recently there has been a big deal of attention on the surface segregation due to conformational asymmetry of the molecules of the polymer blend and due to differences in topology [4,8–17]. It was established that the composition of polymer blends in the vicinity of surfaces can be different

from the bulk composition even for neutral surfaces. It was found that for polymer blends composed of polymers with different degree of polymerization but of chemically identical monomers, shorter polymers are in excess at the wall. It was also demonstrated in simulations [4,11] and supported by calculations using the integral equation theory [18] that stiffer polymers are present in excess in the vicinity of the wall. However the self-consistent field theory developed in Ref. [13] predicts the opposite effect, i.e., the excess of more flexible polymers. Unfortunately, no predictions on the behavior of polymer blends of chemically identical polymers with different degrees of polymerization were made in Ref. [13].

In this paper we present the analytical study of the behavior of athermal polymer blend in the presence of a hard wall using the generalization of the Edwards' collective description of dense polymer systems in terms of effective potentials [19,20] to polymer blends in the presence of a neutral surface. The bare one-polymer Green's function  $G$  obeys the Dirichlet boundary condition. We show that a partial summation of graphs results in replacing the bare  $G$  with the effective one-polymer Green's function  $G_r$ , which, as we argue, obeys the reflecting boundary condition. The bare and effective Green's functions are related by the Dyson equation, where the self-energy  $\Sigma$  is defined by series of graphs. This part of our work is similar to Ref. [13], however with the following significant difference. In the present work the Dyson equation results in an integral equation for  $G_r$ , which determines the relevant reference state to describe polymer melts in the presence of a neutral wall. The concentration profiles are due to fluctuations, which are not taken into account in self-consistent field theories. The method we use can be applied in a straightforward way to study the behavior of polymer blends and copolymer melt in the presence of selective surfaces, the dimensions of polymer molecules in the melt, the distribution of polymer ends, etc.

The paper is organized as follows. Section II A outlines the statistics of a single polymer chain in the presence of a hard wall. Section II B introduces to the collective description of dense polymer system. Section II C contains the discussion of the behavior of the effective potentials and screening effects in the presence of a hard wall. Section II D introduces to the collective description in the presence of a

neutral surface. Section III contains calculations of the excess monomer concentration of constituents of an incompressible athermal polymer blend in the vicinity of a hard wall. Section IV contains our conclusions.

## II. COLLECTIVE DESCRIPTION OF DENSE POLYMER SYSTEMS

### A. Polymer chains in the presence of a hard wall

The Green's function of a free polymer, which is proportional to the relative number of configurations of the ideal chain with the ends fixed at  $\mathbf{r}$  and  $\mathbf{r}'$ , and gives under appropriate normalization the distribution function of the end-to-end distance, obeys the Schrödinger type differential equation [19,21]

$$\left[ \frac{\partial}{\partial N} - a^2 \nabla_{\mathbf{r}}^2 \right] G(\mathbf{r}, N; \mathbf{r}') = \delta(\mathbf{r} - \mathbf{r}') \delta(N), \quad (1)$$

where  $N$  is the number of statistical segments, and  $a^2 = l^2/6$  with  $l$  being the statistical segment length of the chain. The distribution function of the end-to-end distance obtained from Eq. (1) reads

$$G_0(r, N; 0) = \left( \frac{1}{4\pi a^2 N} \right)^{3/2} \exp\left(-\frac{r^2}{4a^2 N}\right). \quad (2)$$

In the presence of a hard wall we have to impose an appropriate boundary condition on Eq. (1). For polymers in a dilute solution with a hard wall situated at  $z=0$  one should use the Dirichlet boundary condition

$$G(\mathbf{r}, N; \mathbf{r}')|_{z=0} = 0, \quad (3)$$

where  $\mathbf{r} \equiv \{\mathbf{r}_{\parallel}, z\}$ . The solution of Eq. (1) with the boundary condition (3) is given by

$$G(\mathbf{r}, N; \mathbf{r}') = G_0(\mathbf{r}_{\parallel} - \mathbf{r}'_{\parallel}, N; 0) [G_0(z - z', N; 0) - G_0(z + z', N; 0)]. \quad (4)$$

It was argued in Ref. [22] that for an incompressible polymer melt in the presence of a neutral surface one should impose the reflecting (Neumann) boundary condition

$$\partial_z G(z, N; z')|_{z=0} = 0 \quad (5)$$

on the Green's function of single polymer chains. The solution of Eq. (1) with the boundary condition (5) is given by

$$G(\mathbf{r}, N; \mathbf{r}') = G_0(\mathbf{r}_{\parallel} - \mathbf{r}'_{\parallel}, N; 0) [G_0(z - z', N; 0) + G_0(z + z', N; 0)]. \quad (6)$$

The Laplace transform of the  $z$  part of the Green's function with respect to  $N$ , which we will need in the following, is given by

$$G_0(z - z', p) = \frac{1}{2a\sqrt{p}} \exp\left(-|z - z'| \frac{\sqrt{p}}{a}\right). \quad (7)$$

The monomer density of a single polymer chain

$$n(z, N) = \int_0^N ds \langle \delta(z - z(s)) \rangle \quad (8)$$

can be expressed through the Green's function of the polymer chain as follows

$$n(z, N) = \int_0^N ds \int_0^\infty dz' \int_0^\infty dz'' G(z', z, N-s) G(z, z'', s). \quad (9)$$

The straightforward computation using the Green's function obeying adsorbing and reflecting boundary condition yields

$$n(z, N) = N \left[ 2 \operatorname{erf}(z/2) + z^2 [1 + \operatorname{erf}(z/2)] + \frac{2z}{\sqrt{\pi}} \exp(-z^2/4) - \operatorname{erf}(z) - 2z^2 \operatorname{erf}(z) - \frac{2z}{\sqrt{\pi}} \exp(-z^2) \right], \quad (10)$$

$$n(z, N) = N, \quad (11)$$

respectively. The distance  $z$  in Eq. (10) is measured in units of  $R_g$ . The monomer density of one chain in the presence of a hard wall does not depend on the distance to the wall in the case of the reflecting boundary condition. The multiplication of  $n(z, N)$  in Eqs. (10) and (11) with the number of chains per volume  $n/\mathcal{V}$  gives the monomer density of a mixture of independent chains. The necessity of change of the boundary condition in the polymer melt will be discussed at the end of Sec. II D.

### B. Collective description of the polymer mixture in bulk

In the analytical approach to the description of dense polymer systems due to Leibler [5] the random phase approximation is used to derive the Ginzburg-Landau type functional of the diblock copolymer melt as a functional of the order parameter. The collective description of concentrated polymer systems due to Edwards [20] gives the physical quantities under interest as series in powers of the effective potentials. These series are closely related to those in the theory of polymer solutions [23] with the main difference that the bare interaction potentials between the monomers are replaced by the effective ones (see below). The diagrammatic way of introduction the collective description in Ref. [24] enables one to go beyond the random phase approximation and establishes the connection between Leibler's and Edwards' approaches.

We now will consider the collective description of the polymer mixture consisting of  $A$  and  $B$  polymers in terms of effective potentials following Ref. [24], where this approach was developed for copolymer melt. The elastic part of the Edwards free energy of  $n_A$  polymers of type  $A$  and  $n_B$  polymers of type  $B$  chains confined to a volume  $V$  is given by

$$F_{el} = \frac{3}{2l^2} \sum_{m=1}^{n_A+n_B} \int_0^N ds \left( \frac{d\mathbf{r}_m(s)}{ds} \right)^2, \quad (12)$$

where  $\mathbf{r}_m(s)$  parametrizes the configuration of  $m$ th polymer as a function of the position along the chain  $s$ . The interac-

tion part of the free energy (in units of  $k_B T$ ) of the blend can be written using the microscopic monomer densities of both polymers

$$\rho_A(\mathbf{r}) = \sum_{m=1}^{n_A} \int_0^N ds \delta[\mathbf{r} - \mathbf{r}_m(s)],$$

$$\rho_B(\mathbf{r}) = \sum_{m=n_A+1}^{n_A+n_B} \int_0^N ds \delta[\mathbf{r} - \mathbf{r}_m(s)] \quad (13)$$

in the form

$$F_{\text{int}} = \frac{1}{2} \int d^3 r_1 \int d^3 r_2 \rho_\alpha(\mathbf{r}_1) V_{\alpha\beta}(\mathbf{r}_1 - \mathbf{r}_2) \rho_\beta(\mathbf{r}_2), \quad (14)$$

where

$$V_{\alpha\beta}(\mathbf{r}_1 - \mathbf{r}_2) = \begin{pmatrix} V & V + \chi \\ V + \chi & V \end{pmatrix} \delta^{(3)}(\mathbf{r}_1 - \mathbf{r}_2). \quad (15)$$

( $\alpha, \beta = A, B$ ) is the interaction matrix of monomer-monomer interactions, and  $\chi$  is connected to the Flory-Huggins parameter. The sum convention over repeated indices is implied in Eq. (14) and henceforth.

Let us now start with the computation of the average concentration of one of the polymers

$$\langle \rho_\alpha(\mathbf{r}) \rangle = \frac{\int Dr_i(s) \rho_\alpha(\mathbf{r}) \exp(-F_{\text{el}} - F_{\text{int}})}{\int Dr_i(s) \exp(-F_{\text{el}} - F_{\text{int}})}, \quad (16)$$

using the collective description of the polymer blend in terms of effective potentials. The average monomer density can be written after introducing a two-component field  $\Phi_\alpha(r)$  in the equivalent form as follows

$$\langle \rho_\alpha(\mathbf{r}) \rangle = \frac{\int Dr_i(s) \int D\Phi(\mathbf{r}) \prod_{\mathbf{r}', \beta} \delta(\Phi_\beta - \rho_\beta) \Phi_\alpha(\mathbf{r}) e^{-F_{\text{el}} - F_{\text{int}}}}{\int Dr_i(s) \int D\Phi(\mathbf{r}) \prod_{\mathbf{r}', \beta} \delta(\Phi_\beta - \rho_\beta) e^{-F_{\text{el}} - F_{\text{int}}}}. \quad (17)$$

The insertion of the Fourier transformation of the infinite product of  $\delta$ -functions

$$\prod_{\mathbf{r}', \beta} \delta[\Phi_\beta(\mathbf{r}') - \rho_\beta(\mathbf{r}')] = \int DQ(\mathbf{r}) e^{iQ(\Phi - \rho)}$$

into Eq. (17), and replacement the order of integrations over the fields  $\Phi(\mathbf{r})$  and  $Q(\mathbf{r})$  with the average over polymer configurations  $\mathbf{r}_i(s)$ , yields the average over polymer configurations in the form

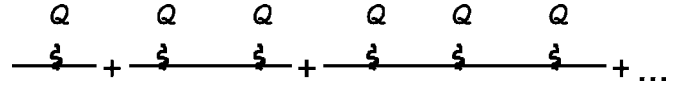


FIG. 1. Examples of graphs associated with the expression (20).

$$\langle \rho_\alpha(\mathbf{r}) \rangle = \frac{\int D\Phi(\mathbf{r}) \Phi_\alpha(\mathbf{r}) e^{-F_{\text{int}}} \int DQ(\mathbf{r}) e^{iQ\Phi} \langle e^{-iQ\rho} \rangle_0}{\int D\Phi(\mathbf{r}) e^{-F_{\text{int}}} \int DQ(\mathbf{r}) e^{iQ\Phi} \langle e^{-iQ\rho} \rangle_0}, \quad (18)$$

where  $Q\rho$  stands for  $\int d^3 r Q_\alpha(\mathbf{r}) \rho_\alpha(\mathbf{r})$ , and the brackets  $\langle \cdots \rangle_0$  means the average over conformations of ideal polymer chains according to

$$\langle e^{-iQ\rho} \rangle_0 = \int Dr_i(s) e^{-iQ\rho} e^{-F_{\text{el}}}. \quad (19)$$

To perform the average over polymer configurations we expand the first exponent in expression (19) in Taylor series. The mean value (19) decomposes as products of averages over single polymer chains, which have the structure

$$\int d^3 r_1 \cdots \int d^3 r_k Q_\alpha(\mathbf{r}_1) \cdots Q_\alpha(\mathbf{r}_k) \langle \rho_\alpha(\mathbf{r}_1) \cdots \rho_\alpha(\mathbf{r}_k) \rangle, \quad (20)$$

where  $k=0, 1, \dots$ , and  $\alpha=A, B$ . According to Ref. [24] it is convenient to associate expression (20) with a graph containing  $k$  wavy legs, which are associated with  $Q_\alpha(\mathbf{r}_i)$ . An example of graphs with  $k=1, 2, 3$  is shown in Fig. 1. The continuous lines are associated with the propagator (2) for a polymer blend in bulk and (4) for a polymer blend in the presence of a hard wall, respectively. Consequently, the series (19) is associated with a product of  $n_A$  lines for  $A$  polymers and  $n_B$  lines for  $B$  polymers containing an arbitrary number of wavy legs in each line. Note that below we will consider the mean value (19) in the thermodynamic limit  $n_A \rightarrow \infty, n_B \rightarrow \infty, \mathcal{V} \rightarrow \infty$  under the condition that the monomer densities computed using the one-polymer Green's function are constant

$$\langle \rho_\alpha(\mathbf{r}) \rangle_0 = N_\alpha n_\alpha / \mathcal{V} \equiv \rho_\alpha. \quad (21)$$

The corresponding density-density correlator reads

$$\langle \rho_\alpha(\mathbf{r}_2) \rho_\alpha(\mathbf{r}_1) \rangle_0 = \frac{1}{2} \rho_\alpha S_{\alpha\alpha}(r_1 - r_2).$$

It is convenient to introduce the diagonal matrix  $S_{\alpha\beta}$  such that the Fourier transforms of the diagonal elements,  $S_{\alpha\alpha}(k)$ , are the bulk structure factor of the  $\alpha$ th component, which are given by

$$S_{\alpha\alpha}(k) = \rho_\alpha N_\alpha g(k^2 R_{g,\alpha}^2), \quad (22)$$

with  $g(y) = 2/y^2 [\exp(-y) + y - 1]$  being the Debye function.

In order to carry out integrations over the two-component field  $Q(\mathbf{r})$  in treating a blend in bulk [24] one performs a partial summation of the series (19) (the latter can be carried out only in the thermodynamic limit) by taking into account

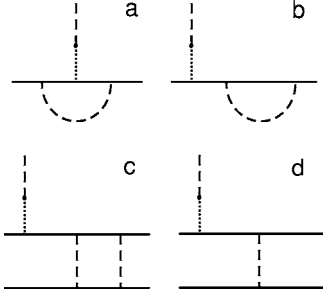


FIG. 2. Examples of graphs contributing to the monomer concentration: graphs *a* and *b* are first order and *c* is second order in  $V^{\text{eff}}$ . After renormalization the continuous line is associated with the effective propagator. Graph *d* with only one insertion of  $V^{\text{eff}}$  is identically zero after renormalization of internal lines.

only the lines with one and two insertions (wavy legs in Fig. 1) in one polymer line. As a result one obtains the expression

$$\exp\left[iQ(\Phi - \langle\rho\rangle_0) - \frac{1}{2}QSQ\right], \quad (23)$$

where  $\langle\rho_\alpha\rangle_0$  is the average monomer density (21). The integrations over  $Q$  for a polymer blend in the bulk is easily performed in Fourier space and result in

$$\exp\left(-\frac{1}{2}\delta\Phi S^{-1}\delta\Phi\right), \quad (24)$$

where  $\delta\Phi(\mathbf{r}) = \Phi(\mathbf{r}) - \langle\rho\rangle_0$ . The expression obtained after performing integrations over  $Q(\mathbf{r})$  can be written as  $\exp(-H\{\delta\Phi\})$  with  $H\{\delta\Phi\}$  being the Ginzburg-Landau functional [5,24].

According to Ref. [24] the functional integration over  $\delta\Phi$  in Eq. (17) yields the monomer density  $\langle\rho_\alpha(\mathbf{r})\rangle$  as a series, which can be associated with Feynman graphs similar to those in the theory of polymer solutions in good solvent (see, for example, Ref. [23]) with the difference that the bare potentials are replaced by the effective ones

$$V^{\text{eff}} = (V^{-1} + S)^{-1}. \quad (25)$$

The lowest-order corrections to the monomer density are depicted in Fig. 2. The external lines in these graphs are associated with the expression

$$V^{\text{ext}} = (V + S^{-1})^{-1}S^{-1}, \quad (26)$$

which can be written in the form  $V^{-1}V^{\text{eff}}$ . The continuous lines denote the bare bulk one-polymer Green's functions (2).

### C. Screened effective potentials in an incompressible polymer blend

We now will consider in more details the properties of the effective potential (25). We remind the reader that the quantities  $S$ ,  $V$ , and  $V^{\text{eff}}$  in Eq. (25) are matrices. The elements of the matrix  $V^{\text{eff}}$  are explicitly given by

$$V_{AA}^{\text{eff}}(k) = \mathcal{R}(k)[-V + 2V\chi S_{BB} + \chi^2 S_{BB}],$$

$$V_{AB}^{\text{eff}}(k) = V_{BA}^{\text{eff}}(k) = -\mathcal{R}(k)[V + \chi],$$

$$V_{BB}^{\text{eff}}(k) = \mathcal{R}(k)[-V + 2V\chi S_{AA} + \chi^2 S_{AA}], \quad (27)$$

where for the sake of simplicity we have introduced the notation

$$\mathcal{R}(k) = [-1 - VS_{AA} - VS_{BB} + 2V\chi S_{AA}S_{BB} + \chi^2 S_{AA}S_{BB}]^{-1}. \quad (28)$$

The behavior of the effective potentials in polymer blends was studied in Refs. [25–27]. In the following we will consider an incompressible and athermal polymer blend, which in the formalism under consideration is described in the limit  $V \rightarrow \infty$  and  $\chi \rightarrow 0$ . The effective potentials (27) simplify in this limit to

$$V_{\alpha\beta}^{\text{eff}}(k) = \frac{1}{S_{AA} + S_{BB}}.$$

Using the explicit expression of the structure factor (22) we obtain for large polymer chains

$$V_{\alpha\beta}^{\text{eff}}(k) = \frac{1}{12} \frac{1}{\rho_A/l_A^2 + \rho_B/l_B^2} k^2. \quad (29)$$

As it follows from Eq. (29) the expansion in powers of effective potentials is in fact an expansion in inverse powers of the density.

We now will consider in more details the properties of the external potentials (26) associated with external lines in graphs *a*, *b*, and *c* in Fig. 2, which are explicitly given by

$$V_{AA}^{\text{ext}}(k) = -\mathcal{R}(k)[1 + VS_{BB}],$$

$$V_{AB}^{\text{ext}}(k) = \mathcal{R}(k)[S_{AA}(V + \chi)],$$

$$V_{BA}^{\text{ext}}(k) = \mathcal{R}(k)[S_{BB}(V + \chi)],$$

$$V_{BB}^{\text{ext}}(k) = -\mathcal{R}(k)[1 + VS_{AA}].$$

In the case of athermal polymer blends the following identities hold

$$V_{AA}^{\text{ext}}(k) - V_{AB}^{\text{ext}}(k) = 1, \quad V_{BB}^{\text{ext}}(k) - V_{BA}^{\text{ext}}(k) = 1. \quad (30)$$

For incompressible and athermal polymer blends  $V_{\alpha\beta}^{\text{ext}}(k)$  simplify to

$$V_{AA}^{\text{ext}}(k) = \frac{S_{BB}}{S_{AA} + S_{BB}}, \quad V_{AB}^{\text{ext}}(k) = -\frac{S_{AA}}{S_{AA} + S_{BB}}.$$

For large polymer chains we finally get

$$V_{AA}^{\text{ext}}(k) = \frac{\rho_B/l_B^2}{\rho_A/l_A^2 + \rho_B/l_B^2}, \quad V_{AB}^{\text{ext}}(k) = -\frac{\rho_A/l_A^2}{\rho_A/l_A^2 + \rho_B/l_B^2},$$

and similar for  $V_{BA}^{\text{ext}}(k)$  and  $V_{BB}^{\text{ext}}(k)$ . Note that in this limit the external lines are independent of the wave number  $\mathbf{k}$ . Therefore, in the real space the external potential are local and are given by the Dirac's  $\delta$ -function in this limit.

### D. Collective description of the polymer mixture in the presence of a hard wall

We now will consider the collective description of a polymer blend in the presence of a hard wall. In contrast to the

collective description of polymer blend in the bulk outlined in Sec. II B we have to use now instead of the free propagator given by Eq. (2) a propagator fulfilling an appropriate boundary condition. In a theory based on the statistical-mechanical description of single polymer chains, the boundary conditions should coincide with those of single polymers, i.e., be the Dirichlet boundary condition (3). Since the behavior of a polymer chain in solution and in a polymer melt in the presence of a wall may be quite different, one can expect that the one-polymer Green's functions in solution and in melt may obey different boundary conditions. A consistent statistical-mechanical theory of polymer melt should be able, in principle, to derive the boundary condition for one-polymer Green's function appropriate for melt. We will show here that using a partial summation of graphs it is possible to reformulate the description of polymer blend in terms of the effective one-polymer Green's function. We will bring forward the arguments that the latter should obey the reflecting boundary conditions.

In order to introduce the collective description in the presence of the wall, we perform the same steps as in the bulk and arrive at the expression (18), and expand further  $\langle \exp(-iQ\rho) \rangle_0$  in Taylor series as given in Eq. (20). In contrast to the bulk the continuous lines are associated with bare one-polymer Green's functions obeying the Dirichlet boundary condition (3). The field  $\Phi_\alpha(\mathbf{r})$  as well as  $Q_\alpha(\mathbf{r})$  are defined in the whole space as in the bulk formalism. The mean density obtained by using the adsorbing boundary conditions is given by Eq. (10) multiplied with the factor  $n_\alpha/\mathcal{V}$ . The computation of the density-density correlation function  $\langle \rho_\alpha(r_1)\rho_\alpha(r_2) \rangle_0$  (no summation over  $\alpha$ ) for a polymer blend in the presence of a hard wall gives

$$\begin{aligned} \langle \rho_\alpha(\mathbf{r}_2)\rho_\alpha(\mathbf{r}_1) \rangle_0 &= \frac{1}{2}\rho_\alpha \int_0^N ds_2 \int_0^{s_2} ds_1 \langle \delta[z_2 - z(s_2)] \\ &\quad \times \delta[z_1 - z(s_1)] \delta[\mathbf{r}_{2,\parallel} - \mathbf{r}_{2,\parallel}(s_2)] \\ &\quad \times \delta[\mathbf{r}_{1,\parallel} - \mathbf{r}_{2,\parallel}(s_1)] \rangle_0 \\ &= \frac{1}{2}\rho_\alpha \int_{k_\parallel} \exp[ik_\parallel(\mathbf{r}_{2,\parallel} - \mathbf{r}_{1,\parallel})] S_{\alpha\alpha}(z_2, z_1, k_\parallel, N), \end{aligned} \quad (31)$$

where the Laplace transform of the diagonal element of the structure factor is given by

$$S_{\alpha\alpha}(z_2, z_1, k_\parallel, p) = \frac{2}{p^2} [G_0(z_2 - z_1, p + x) - G_0(z_2 + z_1, p + x)], \quad (32)$$

and where the notation  $x = k_\parallel^2 a^2$  has been introduced. The nondiagonal elements of the matrix  $S_{\alpha\beta}$  are zero. Note that mean values of density products are zero if one of  $z_i$  is negative, so that the expression (32) applies only for positive  $z_1$  and  $z_2$ .

For a polymer blend in the presence of a wall the translationally invariant part of the structure factor (32) is defined only in the half space, so that the integration over  $Q$ , which



FIG. 3. Vertex with two insertions generated by the second term of Eq. (33).

requires the inversion of  $S_{\alpha\beta}$ , is not so straightforward. In this case we separate the density-density correlator in two parts according to

$$\begin{aligned} \langle \rho_\alpha(\mathbf{r}_2)\rho_\alpha(\mathbf{r}_1) \rangle_0 &= \langle \rho_\alpha(\mathbf{r}_2)\rho_\alpha(\mathbf{r}_1) \rangle_{0b} + \langle \rho_\alpha(\mathbf{r}_2)\rho_\alpha(\mathbf{r}_1) \rangle_0 \\ &\quad - \langle \rho_\alpha(\mathbf{r}_2)\rho_\alpha(\mathbf{r}_1) \rangle_{0b} \\ &= \langle \rho_\alpha(\mathbf{r}_2)\rho_\alpha(\mathbf{r}_1) \rangle_{0b} + \langle \rho_\alpha(\mathbf{r}_2)\rho_\alpha(\mathbf{r}_1) \rangle_{0s}, \end{aligned} \quad (33)$$

and perform a partial summation by taking into account in every line only the first term in Eq. (33). In proceeding in this way we fix the reference state to be that of the bulk far from the wall. The prize to pay is that the 2nd term in Eq. (33) has to be taken into account as a vertex with two insertions, which is shown in Fig. 3.

The summation over lines with one and two insertions in one line results exactly in the expression given by Eq. (23) with the average density given now by Eq. (10). The terms in the series (19) with more than two fields  $Q(\mathbf{r})$  along one line [and two fields corresponding to the 2nd term in Eq. (33)] can be obtained from Eq. (23) and consequently Eq. (24) as derivatives with respect to  $\delta\Phi(\mathbf{r})$ . To compute the concentration profile according to Eq. (17) one should perform integration over the field  $\Phi(\mathbf{r})$ . While after integrations over  $Q$  the series (19) depends on  $\delta\Phi(\mathbf{r}) = \Phi(\mathbf{r}) - \langle \rho \rangle$ , the interaction part of the free energy (14) has the form  $F_{\text{int}} = \frac{1}{2}\Phi V \Phi$ . Rewriting the latter in terms of  $\delta\Phi$  yields

$$F_{\text{int}} = \frac{1}{2}\delta\Phi V \delta\Phi + \delta\Phi V \langle \rho \rangle, \quad (34)$$

where the linear term in  $\delta\Phi$  has the same form as interaction with an external field in the formalism of  $\Phi^4$  theory. For an incompressible and athermal polymer blend, which we consider in the present work, the linear term vanishes.

Similar to the consideration in bulk the expression obtained after performing integrations over  $Q(\mathbf{r})$  can be written as  $\exp(-H\{\delta\Phi\})$  with  $H\{\delta\Phi\}$  being a Ginzburg-Landau Hamiltonian including the surface terms. However, in contrast to the effective surface Hamiltonian used in many studies [1] the corresponding terms are not localized at the surface only [28]. The integration over the field  $\Phi(r)$  can be performed in the same way as for bulk.

The collective description developed above is based on the concept of the effective potential, which takes into account the screening of monomer-monomer interactions in a melt. However, the effect of the wall is taken into account as in the case of diluted polymers via the Dirichlet boundary condition for one-polymer Green's function and leads to an inhomogeneous monomer density for distances up to the gyration radius. However, in a melt the density is expected to be rather homogeneous at distances  $z < R_g$ . This is the result of the interplay of the interaction with the wall and the in-

compressibility of the polymer melt. While in the polymer solution (which is a liquid and as such is incompressible) the entropic repulsion with the wall favor the presence of solvent molecules at the wall. In the case of the melt this is not anymore the case, because the place of monomers being repulsed from the wall, will be occupied by monomers belonging to another polymer which at that moment are not or less repulsed from the wall. Due to this the melt density similar to the total density of the solution will not tend to zero in approaching the surface. We expect that the effect of the wall on the behavior in the polymer melt can be formulated in terms of the renormalized one-polymer Green's function, which should guarantee the uniformity of the density, and according to this should obey a boundary condition, which is different from the Dirichlet boundary condition. We now show that, indeed, the partial summation of graphs including insertions into continuous lines enables one to formulate the description of a polymer melt in terms of the effective one-polymer Green's function. We will consider for simplicity the renormalization of the bare one-polymer Green's functions in the expression for the concentration profile

$$\langle \rho_\alpha(z) \rangle = n_\alpha \int_0^{N_\alpha} ds \int_0^\infty dz' G(z', z, N_\alpha - s) \int_0^\infty dz'' G(z, z'', s), \quad (35)$$

where the bare one-polymer propagator obeys the Dirichlet boundary condition. The graphs *b* and *c* in Fig. 2 contribute to the bare Green's functions in (35). Using property (30) and expressing the external potentials  $V_{AA}^{\text{ext}}$  as  $1 + V_{AB}^{\text{ext}}$  we can divide this contribution into two parts. The first one is given by graphs *b* and *c*, in which the external line associated with 1 and which renormalizes the one-polymer propagators in (35). The second part, with the external line associated with  $V_{AB}^{\text{ext}}$ , together with the graph *a* describes the fluctuations corrections to the concentration profile. The renormalization to the first order can be extended to higher orders, with the result that the bare continuous lines will be replaced by the effective ones associated with the effective one-polymer Green's function. This procedure corresponds to reduction of the whole set of graphs to the skeleton graphs, i.e., the graphs without insertions into internal lines. The only exception are the graphs *b* and *c* in Fig. 2, which are due to the recasting of  $V_{AA}^{\text{ext}}$ . The renormalization of one-polymer graphs due to insertions into the internal lines can be represented using the Dyson equation

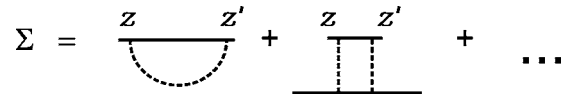


FIG. 4. The lowest-order graphs contributing to the self-energy. The continuous lines are associated with the effective one-polymer propagator  $G_{r,\alpha}$ .

$$G_r^{-1} = G^{-1} - \Sigma, \quad (36)$$

where  $\Sigma$  is the self-energy, which takes into account insertions along the chain. Note that  $G$ , etc., in Eq. (36) are matrices with respect to spatial coordinates. Examples of graphs contributing to  $\Sigma$  are given in Fig. 4.

As a result of the partial summation of graphs taking into account the insertions into internal lines according to Eq. (36) the lowest-order contribution to the density profile (35) changes to

$$\langle \rho_\alpha(z) \rangle = n_\alpha \int_0^{N_\alpha} ds \int_0^\infty dz' G_{r,\alpha}(z', z, N_\alpha - s) \times \int_0^\infty dz'' G_{r,\alpha}(z, z'', s). \quad (37)$$

The fluctuation corrections to Eq. (37) are given by the skeleton graphs in Figs. 2 and 5. As a result of the partial summation the bare one-polymer propagators  $G$  are replaced by the effective ones  $G_{r,\alpha}$ .

Equation (36) with  $\Sigma$  given as an infinite set of graphs is the basis of the self-consistent computation of the effective one-polymer Green's function in the polymer blend under presence of a hard wall. The solution of this equation is a difficult task which goes beyond the scope of the present article.

Fortunately, the form of  $G_{r,\alpha}$  in polymer fluid can be found from general arguments avoiding the direct solution of Eq. (36). According to the above discussion we expect that the density profile in an incompressible fluid in the presence of neutral wall will be uniform. On the another hand the density profile without taking into account the fluctuations is given by Eq. (37). As we have shown in Sec. II A the computation of the density using the one-polymer Green's function obeying the reflecting boundary condition gives a homogeneous density. Due to this we identify the effective one-polymer propagators  $G_{r,\alpha}$  with that obeying the reflecting

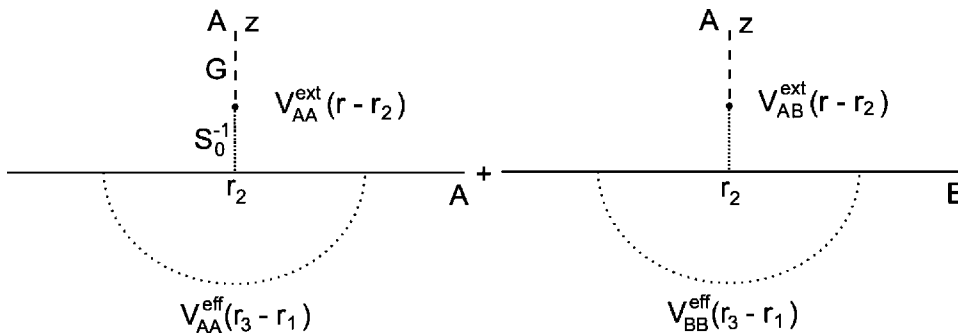


FIG. 5. The Feynman diagrams giving the leading contribution to the excess monomer concentration.

boundary condition. Deviations from Silberberg hypothesis in thin polymer films were studied recently in Refs. [29–32].

Figure 4 shows that the contributions to the self-energy does not reduce to an effective potential as it was assumed in Ref. [13] in the approach based on the self-consistent field theory. While the first graph in Fig. 4 takes into account the monomer-monomer interactions along one polymer, the 2nd graph (and higher-order graphs) takes into account monomer-monomer interactions between different polymers. Since the graphs contributing to the self-energy take into account the many particle interactions characteristic for a melt, we expect that the effective one-polymer Green's function  $G_{r,\alpha}$  obeys the boundary conditions appropriate for an incompressible liquid, i.e., the reflecting boundary conditions. This conclusion is supported by the following argument. In polymer melts similar to semidilute polymer solutions the relevant quantity governing the properties of the system is the number of monomers between two subsequent cross-links along the chain, which for polymer melts is of order of unity, instead of the chain length  $N$ . Consequently, in the polymer melt the effect of the wall on the monomers, which are close to the wall, will be similar to that on solvent molecules in solution. However, the monomers are classical objects, which are described in the relaxational regime. For a single monomer (or a solvent molecule), which dynamics is described by the Langevin equation, the steady-state distribution function is given by Boltzmann distribution  $\exp[-U(z)/k_B T]$  and is therefore constant in the space between two walls. This makes clear that the Dirichlet boundary condition is irrelevant in dense polymeric systems.

It is well known that a polymer configuration corresponds to the trajectory of a quantum particle for imaginary times. According to this the problem of boundary condition in polymer melts is expected to have its counterpart in quantum fluids in the presence of a neutral boundary. While the wave functions of single particles obey the Dirichlet boundary condition at the wall, the density of the fluid is not required to be zero at the wall [33].

### III. COMPUTATION OF THE EXCESS MONOMER CONCENTRATION

The skeleton graphs in Fig. 2 give the fluctuational part to the density profile. The free end of the external line is associated with the argument of the monomer density  $z$  (due to the symmetry along the wall the monomer density does not depend on  $\mathbf{r}_\parallel$ ). The explicit calculation shows that the one-loop graphs, where the external line is located outside the loop (graphs  $b$  and  $c$  in Fig. 2), are negligible for large  $N$ . The leading contribution is due to the graph  $a$  and the related graph, which describes the effect of  $B$  polymers on the concentration of  $A$  polymers. These graphs are shown in more details in Fig. 5.

We now will consider the computation of the concentration of say the component  $A$  in the presence of a hard wall. We will assume that the statistical segment length of the polymer  $A$  is larger than that of the polymer  $B$ ,  $l_A > l_B$ , so that the polymer  $A$  is stiffer. The contribution to the excess concentration to the lowest order in powers of the effective po-

tentials is given by graphs in Fig. 5. To conduct calculations it is convenient to consider the Laplace transform with respect to the contour length  $N$ . The analytical expression associated with the first graph in Fig. 5 is given by

$$-\frac{\rho_A V_{AA}^{\text{ext}}}{8\pi^3 N_A} \int d^2 q_\parallel \int dq V_{AA}^{\text{eff}}(q_\parallel^2 + q^2) \times \frac{q^2 a^2 e^{-2z\sqrt{p+x/a}} + 2qa\sqrt{p+x} \sin(qz) e^{-z\sqrt{p+x/a}} + p+x}{p^2(p+x)(p+x+q^2 a^2)^2}, \quad (38)$$

where  $p$  is Laplace conjugate to  $N$  and  $x=q_\parallel^2 a^2$ . The analytical expression of the 2nd graph in Fig. 5 is obtained from Eq. (38) using the replacements

$$V_{AA}^{\text{ext}} \rightarrow V_{AB}^{\text{ext}}, \quad V_{AA}^{\text{eff}} \rightarrow V_{BB}^{\text{eff}}, \quad \rho_A \rightarrow \rho_B, \quad N_A \rightarrow N_B.$$

Note that the factor  $-1$  is due to the fact that  $V$  and  $V^{\text{eff}}$  appear with the sign minus in the exponential of the statistical weight of polymer configurations. The  $k^2$  dependence of the effective potentials (29) leads to the divergence of the integrals over the wave vector in Eq. (38) at the upper limit of integration. However, the effective potentials acquire for finite  $V$  their bare values for large  $k$ , so that the integral converges at the upper limit of the integration. Therefore, for finite  $V$  the effective potentials are screened only for lengths larger than the local length

$$l_c \approx V^{-1/2} (\rho_A l_A^2 + \rho_B l_B^2)^{-1/2},$$

which is obtained from the explicit expressions of the effective potentials (27). The derivation shows that this length is the same for both polymers. We expect that for finite  $V$  the polymer blend can be considered as an incompressible only for lengths larger than  $l_c$ . In order to simplify the integration over the wave vector in Eq. (38) we use the athermal and incompressible limit of the effective potentials (29), but restrict the integration to wave vectors smaller than the cutoff value  $\Lambda \approx l_c^{-1}$ .

The inspection of Eq. (38) shows that it (and the expression associated with graphs with the external line being outside the loop) contains a  $z$  independent contribution to the excess concentration of the density. The straightforward computation yields the renormalization of the bulk monomer concentration as

$$\tilde{\rho}_A = \rho_A \left[ 1 + (1-2) \frac{3\rho_B \Lambda}{4\pi} \frac{l_A^2 l_B^2}{(\rho_A l_B^2 + \rho_B l_A^2)^2} \left( \frac{1}{l_B^2} - \frac{1}{l_A^2} \right) \right]. \quad (39)$$

The factor 2 in Eq. (39) accounts for graphs similar to the graphs  $b$  and  $c$  in Fig. 2 but with the external lines being on the right side of the interaction line. Note that the mass divergences [23] of the graphs  $b$  and  $c$  are omitted, that implies the regularization of expression (16) with respect to the mass divergences at the beginning. Equation (39) shows that even in the bulk the packing effects change the bare density of the constituents: the concentration of the stiffer polymer becomes smaller. Without incorporating the possibility for a local nematic ordering, which is not taken into account in the

model of a Gaussian polymer chain, polymers with larger statistical segment length are expected to have smaller density. Note that the renormalization of the bulk composition is local, and the comparison of Eq. (39) with the corresponding expression for  $\tilde{\rho}_B$  shows that the total density of the blend does not change. Although the renormalization of the bulk composition given by Eq. (39) is somewhat unexpected, its necessity can be explained qualitatively as follows. The density of an incompressible liquid at given  $T$  and  $\mathcal{V}$  is determined by interactions between the molecules, and cannot be chosen arbitrarily as in gas-like systems. Thus, in application of the coarse-grained model under consideration to polymer blend Eq. (39) describes the renormalization of bare concentrations towards their concentrations in the polymer melt, which are determined by monomer-monomer interactions.

The  $z$  dependent part of Eq. (38) gives the excess monomer concentration as a function of the distance to the wall. The integration over the wave vector yields the simple expression

$$\begin{aligned} & -\frac{V_0}{8a^5 p^2 \pi z} \left[ e^{-(2z/a)\sqrt{p}(a-z\sqrt{p})} - e^{-(2z/a)\sqrt{p+a^2\Lambda^2}} \right. \\ & \times \left( a - \frac{zp}{\sqrt{p+a^2\Lambda^2}} \right) \left. - \frac{V_0\Lambda}{2a^4\pi^2 p^2} \left[ \Gamma_0\left(\frac{2z}{a}\sqrt{p}\right) \right. \right. \\ & \left. \left. - \Gamma_0\left(\frac{2z}{a}\sqrt{p+a^2\Lambda^2}\right) \right] \right], \end{aligned} \quad (40)$$

where  $\Gamma_\alpha(x) = \int_x^\infty dt t^{\alpha-1} \exp(-t)$  is the incomplete  $\gamma$  function, and the notation

$$V_0 = \frac{1}{12} \frac{\rho_A \rho_B}{N_A l_B^2 (\rho_A l_A^2 + \rho_B l_B^2)^2}$$

is introduced. To obtain the excess density one should add to expression (40), which is associated with the first graph in

Fig. 5, the corresponding expression associated with the 2nd graph in Fig. 5.

We will first compute the excess concentration of the stiffer ( $A$ ) polymer at the surface  $\delta\rho_A(z=0)$ . To that end we put  $z=0$  in Eq. (40), take into account the second graph in Fig. 5, and perform the inverse Laplace transform. For large  $N$  we obtain the result

$$\begin{aligned} \delta\rho_A(z=0) = \frac{3}{4\pi^2} \Lambda \frac{\rho_A \rho_B l_A^2 l_B^2}{(\rho_A l_B^2 + \rho_B l_A^2)^2} & \left[ \frac{1}{l_B^2} \ln(a_B^2 \Lambda^2 N_B) \right. \\ & \left. - \frac{1}{l_A^2} \ln(a_A^2 \Lambda^2 N_A) \right]. \end{aligned} \quad (41)$$

If both polymers have the same gyration radius  $R_g = a\sqrt{N}$  Eq. (41) simplifies to

$$\delta\rho_A(z=0) = \frac{3}{4\pi^2} \Lambda \frac{\rho_A \rho_B l_A^2 l_B^2}{(\rho_A l_B^2 + \rho_B l_A^2)^2} \left( \frac{1}{l_B^2} - \frac{1}{l_A^2} \right) \ln(\Lambda^2 R_g^2). \quad (42)$$

The excess concentration at the wall for polymer blend differing only in degrees of polymerization is derived from Eq. (41) as

$$\delta\rho_A(z=0) = \frac{3}{4\pi^2} \frac{\Lambda}{l^2} \frac{\rho_A \rho_B}{(\rho_A + \rho_B)^2} \ln \frac{N_B}{N_A}.$$

The latter shows that the shorter polymers are present in excess at the wall. Notice that the excess concentration depends logarithmically on the number of segments  $N$ . The contribution to the excess concentration at  $z=0$  associated with graphs  $b$  and  $c$  in Fig. 2 reads

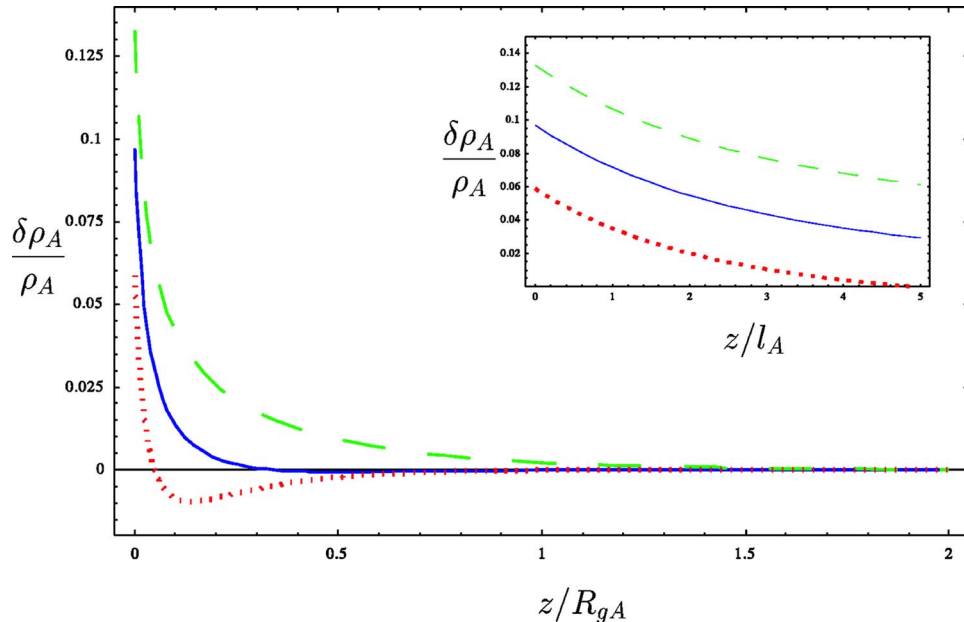


FIG. 6. (Color online) Concentration profile of  $A$  polymers as a function of the distance to the surface for different values of  $N_B$ , and  $l_A=1.5$ ,  $l_B=1$ ,  $\Lambda^{-1}=1.55$ ,  $\rho_A=\rho_B=0.5$ . The continuous line:  $N_A=N_B=10^4$ ; dashes:  $N_B=5 \times 10^4$ ; dots:  $N_B=2 \times 10^3$ . The inset shows the concentration profile in the vicinity of the surface as a function of the distance measured in units of  $l_A$ .



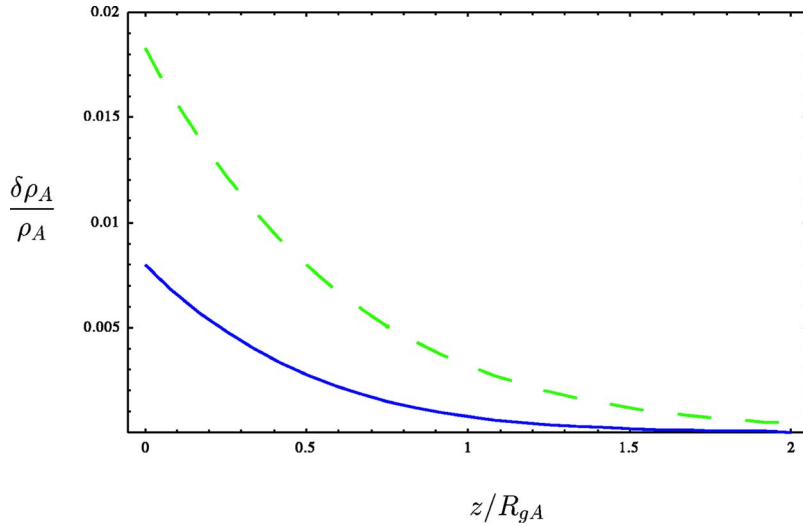


FIG. 7. (Color online) Concentration profile of A polymers as a function of the distance to the surface for different values of  $N_B$ , and  $l_A=l_B=1.5$ ,  $N_A=10^4$ ,  $\Lambda^{-1}=1.55$ ,  $\rho_A=\rho_B=0.5$ . The continuous line:  $N_B=2 \times 10^4$ ; dashes:  $N_B=5 \times 10^4$ .

$$\delta\rho_A(z=0) = -\frac{1}{8(6\pi)^{3/2}l_A^2} \frac{\rho_A}{(\rho_A l_B^2 + \rho_B l_A^2)^2} \left[ \frac{l_B^5 \rho_A}{\sqrt{N_A}} \ln\left(\frac{4}{9} a_A^2 \Lambda^2 N_A\right) + \frac{l_A^5 \rho_B}{\sqrt{N_B}} \ln\left(\frac{4}{9} a_B^2 \Lambda^2 N_B\right) \right]. \quad (43)$$

Due to the factor  $N^{-1/2}$  the latter vanishes for large  $N$ . Note that for conformationally asymmetric polymers of the same gyration radius the sign of Eq. (43) is opposite to that of Eq. (42). The increase of  $\delta\rho_A(z=0)$  with  $N$  agrees qualitatively with the results of numerical simulations and calculations using the integral equation theory [4].

To compute  $\delta\rho_A(z)$  for arbitrary  $z$  one should perform the inverse Laplace transform of Eq. (40). Since it cannot be performed analytically, we have used a numerical routine (Durbin) for inverse Laplace transform in Mathematica. The results of the numerical calculation of the excess concentration of stiffer polymers  $\delta\rho_A(z)$  for different values of the degrees of polymerization of more flexible polymer are shown in Fig. 6. It shows that the increase of  $N_B$  results in an increase of the excess concentration of the A polymer. For  $N_B < N_A$  the concentration of A polymers is still in excess in the vicinity of the wall, but becomes lower than in the bulk for intermediate distances, i.e., the B polymers are in excess at these distances. These results are in agreement with numerical simulations and computations using the integral equation theory [4]. Figure 7 shows the result of the computation of the excess concentration of the shorter polymers in a polymer blend consisting of chemically identical polymers, which differ only in their degrees of polymerization. Figure 7 shows that shorter polymers are present in excess in the vicinity of the wall. This finding is in qualitative agreement with the result predicted in Ref. [34] and observed in Refs. [14,35–37].

The excess of shorter polymers in the case under consideration is compatible with the excess of the solvent at the wall in a polymer solution. The latter corresponds to the limit, when the polymerization degree of shorter polymers tends to unity. However, to describe this limit one has to take into account the higher-order terms in the perturbation series for the concentration profile.

Note that the both cases we have considered above ( $l_A \neq l_B$ ,  $R_{gA}=R_{gB}$ , and  $l_A=l_B$ ,  $N_A \neq N_B$ ) follow from the general formula (40).

We now will give a qualitative explanation of the different behavior of polymers in the blend under the influence of a hard wall. A single polymer in a dilute solution obeys the Dirichlet boundary condition. As a consequence of the boundary condition the number of configurations available to the polymer chain lowers with the decrease of the distance to the wall. The latter results in an entropic repulsion of the polymer from the wall, and is responsible for the vanishing of the density at the wall. According to this the solvent molecules are favored in the vicinity of the wall with respect to the polymer monomers. A simple calculation using the distribution function obeying the Dirichlet boundary condition shows that the force acting on the free end of the polymer at a given distance to the wall is controlled by the gyration radius of the polymer  $R_g = a\sqrt{N}$ .

A completely different behavior takes place in the case of incompressible polymer melts, where the entropic repulsion from the wall is balanced by the melt pressure with the consequence that the density is uniform. However, there is a difference in the behavior of the polymers in the vicinity of the wall for melt composed of different polymers. We consider first a polymer blend composed of polymers which differ only in degrees of polymerization. In a layer with the thickness equal to the gyration radius of larger polymers, the larger polymer experiences the entropic force from the wall while the shorter polymer does not. Due to this the larger polymer increases its distance to the wall, which will be occupied by shorter ones, in order that the total density will remain constant. The asymmetry in the behavior of polymers in the vicinity of the wall appears even in a polymer melt composed of identical polymers. According to the above argument the monomers of a polymer coil, which has contacts with the wall, are disfavored with respect to the ends of polymer coils which do not have contacts with the wall. Due to this the polymer ends are expected to be present in excess in the vicinity of the wall. The effect of the distribution of polymer ends on the surface tension was studied in Ref. [38]. A quantitative study of the distribution of polymer ends us-

ing the self-consistent field theory was performed in Ref. [39].

For polymers with different statistical segment lengths, but the same gyration radius the difference in the behavior in the vicinity of the wall can be explained qualitatively as follows. The monomer density of a polymer coil is given by  $\rho_c = N/R_g^3 = a^{-2}/R_g$ , while the surface density of a coil is  $\rho_s = \rho_c R_g = a^{-2}$ . Therefore, the surface density  $\rho_s$  of the stiffer polymer is smaller. It is likely to expect that the repulsive effect of the wall on the coil is proportional to  $\rho_s$ . According to this the repulsive effect of the wall is stronger for more flexible polymers. This is the reason that the monomers of stiffer polymers will be favored in the vicinity of the wall. The surface enrichment  $\delta\rho_A$  is expected to be proportional to the differences of surface densities, i.e.,  $\delta\rho_A \sim \rho_s^B - \rho_s^A$ , which agrees with our quantitative result (42). According to this qualitative consideration the difference in surface densities  $\rho_s^B - \rho_s^A$  is a drive for the conformational asymmetry. Since the monomers within the layer of thickness  $R_g$  are affected by the wall, we expect that the excess concentration will depend on  $R_g$ . However, the logarithmic dependence on  $R_g$  in Eq. (42) is difficult to derive using only the hand wavy arguments.

Note that in the above computation of the excess concentration  $\delta\rho_A(z)$  we have taken into account the lowest-order correction in the series in powers of effective potentials. The effective potentials according to Eq. (29) are inversely proportional to the density, so that the perturbation expansion in powers of effective potentials is a series in inverse powers of the density. However, since the polymer melt has a fixed density, the inverse density is not a small parameter. The magnitude of the first-order correction can be controlled by considering polymers having the same gyration radius and small differences in  $l_A$  and  $l_B$ , or polymers with small differences in  $N_A$  and  $N_B$  for  $l_A = l_B$ . However, it is not clear without explicit computations, if the 2nd order term is smaller than the 1st order one under the above conditions. From the general point of view one would expect the following bounds on the total effect of the perturbation series. As already men-

tioned above for polymers differing only in degrees of polymerization the effect of the whole perturbation series should recover in the limit  $N_A \ll N_B$  the behavior in polymer solutions, where the polymer concentration will tend to zero in approaching the surface. For polymers differing in flexibility the concentration of the stiffer polymer at the wall cannot exceed the total density of the polymer blend in bulk. In other words the concentration of the more flexible polymer cannot be negative. This determines the upper limit of applicability of our results given by Eqs. (41) and (42).

#### IV. CONCLUSIONS

To summarize, we have generalized the Edwards' collective description of dense polymer systems in terms of effective potentials to polymer blends in the presence of a surface. Using this formalism we have studied an incompressible athermal polymer blend of conformationally asymmetric polymers, which differ in statistical segment lengths, in the presence of a hard wall. We have computed the excess concentrations of constituents to the first order in powers of effective potentials. We have found that stiffer polymers are in excess in the vicinity of the surface, and that the concentration excess at the surface depends logarithmically on the degrees of polymerization. For polymer blends differing only in degrees of polymerization the shorter polymers are in excess at the wall. Our results are in agreement with numerical results available in the literature. The present method can be applied in a straightforward way to study the behavior of polymer blends and copolymer melt in the presence of selective surfaces, to study the dimensions of polymer molecules in the melt, the distribution of polymer ends, etc.

#### ACKNOWLEDGMENTS

We would like to thank H. Angerman and A. Johner for useful discussions. A financial support from the Deutsche Forschungsgemeinschaft, SFB 418 is gratefully acknowledged.

- 
- [1] K. Binder, *Acta Polym.* **46**, 204 (1995).
  - [2] G. H. Fredrickson, *Macromolecules* **20**, 2535 (1987).
  - [3] K. Binder, in *Phase Transitions and Critical Phenomena*, edited by C. Domb and J. L. Lebowitz (Academic, New York, 1983).
  - [4] A. Yethiraj, S. K. Kumar, A. Hariharan, and K. S. Schweizer, *J. Chem. Phys.* **100**, 4691 (1994).
  - [5] L. Leibler, *Macromolecules* **13**, 1602 (1980).
  - [6] E. Helfand and Y. Tagami, *J. Chem. Phys.* **56**, 3592 (1972).
  - [7] K. F. Freed, *J. Chem. Phys.* **103**, 3230 (1995).
  - [8] M. D. Foster, M. Sikka, N. Singh, F. S. Bates, S. K. Satija, and C. F. Majkrzak, *J. Chem. Phys.* **96**, 8605 (1992).
  - [9] M. Sikka, N. Singh, A. Karim, F. S. Bates, S. K. Satija, and C. F. Majkrzak, *Phys. Rev. Lett.* **70**, 307 (1993).
  - [10] G. H. Fredrickson and J. P. Donley, *J. Chem. Phys.* **97**, 8941 (1992).
  - [11] A. Yethiraj, *Phys. Rev. Lett.* **74**, 2018 (1995).
  - [12] S. K. Kumar, A. Yethiraj, K. S. Schweizer, and F. A. M. Leermakers, *J. Chem. Phys.* **103**, 10332 (1995).
  - [13] D. T. Wu, G. H. Fredrickson, and J.-P. Carton, *J. Chem. Phys.* **104**, 6387 (1996).
  - [14] D. G. Walton and A. M. Mayes, *Phys. Rev. E* **54**, 2811 (1996).
  - [15] J. P. Donley, D. T. Wu, and G. H. Fredrickson, *Macromolecules* **30**, 2167 (1997).
  - [16] O. N. Tretinnikov and K. Ohta, *Langmuir* **14**, 915 (1998).
  - [17] S. Tripathi and W. G. Chapman, *Phys. Rev. Lett.* **94**, 087801 (2005).
  - [18] A. Yethiraj and C. K. Hall, *J. Chem. Phys.* **95**, 3749 (1991).
  - [19] S. F. Edwards, *Proc. Phys. Soc. Jpn.* **88**, 265 (1966).
  - [20] S. F. Edwards, *J. Phys. A* **8**, 1670 (1975).
  - [21] P. G. de Gennes, *Rep. Prog. Phys.* **32**, 187 (1969).
  - [22] A. Silberberg, *J. Chem. Phys.* **48**, 2835 (1968).

- [23] J. des Cloizeaux and G. Jannink, *Polymers in Solution, Their Modeling, and Structure* (Oxford University Press, Oxford, 1990).
- [24] S. Stepanow, *Macromolecules* **28**, 8233 (1995).
- [25] M. G. Brereton and T. A. Vilgis, *J. Phys. (France)* **50**, 245 (1989).
- [26] T. A. Vilgis and R. Borsali, *Macromolecules* **23**, 3172 (1990).
- [27] I. Y. Erukhimovich *et al.*, *Comput. Theor. Polym. Sci.* **8**, 133 (1998).
- [28] A. A. Fedorenko and S. Stepanow (unpublished).
- [29] A. N. Semenov and A. Johner, *Eur. Phys. J. E* **12**, 469 (2003).
- [30] A. Cavallo, M. Müller, J. P. Wittmer, A. Johner, and K. Binder, *J. Phys.: Condens. Matter* **17**, 1697 (2005).
- [31] N. Rehse, C. Wang, M. Hund, M. Geoghegan, R. Magerle, and G. Krausch, *Eur. Phys. J. E* **4**, 69 (2001).
- [32] W. Zhao, M. H. Rafailovich, J. Sokolov, L. J. Fetters, R. Plano, M. K. Sanyal, S. K. Sinha, and B. B. Sauer, *Phys. Rev. Lett.* **70**, 1453 (1993).
- [33] I. M. Khalatnikov, *An Introduction to the Theory of Superfluidity* (W. A. Benjamin, New York, 1965).
- [34] A. Hariharan, S. K. Kumar, and T. P. Russel, *Macromolecules* **23**, 3584 (1990).
- [35] T. F. Schaub, G. J. Kellog, A. M. Mayes, R. Kulasekera, J. F. Ankner, and H. Kaiser, *Macromolecules* **29**, 3982 (1996).
- [36] P. P. Hong, F. J. Boerio, and S. D. Smith, *Macromolecules* **27**, 596 (1994).
- [37] I. Hopkinson, F. T. Kiff, R. W. Richards, S. Affrossman, M. Hartshorne, R. A. Pethrick, H. Munro, and J. R. P. Webster, *Macromolecules* **28**, 627 (1995).
- [38] P. G. de Gennes, *C. R. Acad. Sci.* **307**, Serie II, 1841 (1988).
- [39] D. T. Wu, G. H. Fredrickson, J.-P. Carton, A. Ajdari, and L. Leibler, *J. Polym. Sci., Part B: Polym. Phys.* **33**, 2373 (1995).